

Review

The Application of Cellulose Nanofibrils in Energy Systems

Ruoyu Li ^{1,2,3}, Dong Tian ^{2,3}, Lei Chen ², Bocheng Zhuang ⁴, Hui Feng ², Qiang Li ², Lianghao Yu ^{4,*} 
and Yihan Ling ^{1,3,*}

- ¹ School of Chemical Engineering and Technology, China University of Mining and Technology, Xuzhou 221116, China; liruoyu@hnnu.edu.cn
² School of Computer Science, Huainan Normal University, Huainan 232001, China; tiandong@mail.ustc.edu.cn (D.T.); leichen@hnnu.edu.cn (L.C.); fh@hnnu.edu.cn (H.F.); liq@hnnu.edu.cn (Q.L.)
³ Anhui Key Laboratory of Low Temperature Co-Fired Material, Huainan Normal University, Huainan 232001, China
⁴ Key Laboratory of Spin Electron and Nanomaterials of Anhui Higher Education Institutes, Suzhou University, Suzhou 234000, China; zbc2497669621@outlook.com
* Correspondence: lhyu@ahszu.edu.cn (L.Y.); lyhy@cumt.edu.cn (Y.L.)

Abstract: Nanocellulose has emerged as a highly promising and sustainable nanomaterial due to its unique structures, exceptional properties, and abundance in nature. In this comprehensive review, we delve into current research activities focused on harnessing the potential of nanocellulose for advanced electrochemical energy storage applications. We commence with a brief introduction to the structural features of cellulose nanofibers found within the cellulose resources' cell walls. Subsequently, we explore various processes that have been investigated for utilizing cellulose in the realm of energy storage. In contrast to traditional binders, we place significant emphasis on the utilization of solid electrolytes and 3D printing techniques. Additionally, we examine different application areas, including supercapacitors, lithium-ion batteries, and Zn-ion batteries. Within this section, our primary focus lies in integrating nanocellulose with other active materials to develop flexible substrates such as films and aerogels. Lastly, we present our perspectives on several key areas that require further exploration in this dynamic research field in the future.

Keywords: cellulose nanofibrils; binder; energy storage device



Citation: Li, R.; Tian, D.; Chen, L.; Zhuang, B.; Feng, H.; Li, Q.; Yu, L.; Ling, Y. The Application of Cellulose Nanofibrils in Energy Systems. *Batteries* **2023**, *9*, 399. <https://doi.org/10.3390/batteries9080399>

Academic Editors: Lin Li and Changshin Jo

Received: 25 June 2023

Revised: 12 July 2023

Accepted: 26 July 2023

Published: 1 August 2023



Copyright: © 2023 by the authors. Licensee MDPI, Basel, Switzerland. This article is an open access article distributed under the terms and conditions of the Creative Commons Attribution (CC BY) license (<https://creativecommons.org/licenses/by/4.0/>).

1. Introduction

As the economy continues to rapidly develop, the demand for energy from human beings is increasing at an alarming rate. This emphasizes the urgent need for the advancement of renewable energy sources to replace conventional ones [1]. In response, various energy conversion and storage devices have emerged, such as fuel cells, alkali metal batteries, and supercapacitors [2–5]. However, one particular innovation that has garnered significant attention in recent years is the utilization of biomass-derived cellulose nanofibrils (CNFs) in the realm of energy conversion and storage [6,7]. CNFs, composed of ultrafine fibers derived from cellulose, the most abundant biopolymer on Earth and a fundamental building block of plant cell walls, hold great potential for numerous applications in this field.

Cellulose, a renewable polysaccharide, is abundantly present in plants and microorganisms. Its chemical formula is $(C_6H_{10}O_5)_n$, and it consists of repeating units of β -D-glucopyranose linked through covalent bonds between the -OH groups of C_4 and C_1 carbon atoms [8]. The structural hierarchy of cellulose varies depending on its source, but can be modified through extraction processes to obtain diverse forms of cellulose [9]. Despite its advantages, natural cellulose fibers possess certain limitations, including poor thermal stability and limited compatibility with hydrophobic polymers. To overcome these challenges, cellulose can be transformed into nano/micro-cellulosic forms or combined with suitable polymers to enhance its desired characteristics [10]. Nanocellulose can be broadly categorized into two primary types: (i) cellulose nanocrystals (CNC) obtained through

acid treatment, and (ii) CNFs primarily produced via mechanical disintegration. These modifications allow for the optimization of cellulose properties and expand its potential applications.

Recently, CNFs have garnered significant attention as a noteworthy nanomaterial due to their exceptional properties and wide-ranging applications in diverse fields, including optically transparent materials, reinforced polymer nanocomposites, biomedicine, energy storage devices, and environmental remediation [11,12]. Derived from renewable biomass sources like cellulose, chitin, and lignin, CNFs are produced using a range of processing techniques. These renewable nanofibers offer immense potential for advancing sustainable technologies and addressing various societal challenges [13–15]. Therefore, cellulose serves as an excellent precursor for the fabrication of carbon-based porous materials or carbon hybrid materials, which can be further functionalized to create high-performance carbon electrodes for energy storage devices. The utilization of nanocellulose in energy storage (Figure 1) has gained significant traction due to the inherent advantages offered by its unique structures and properties.

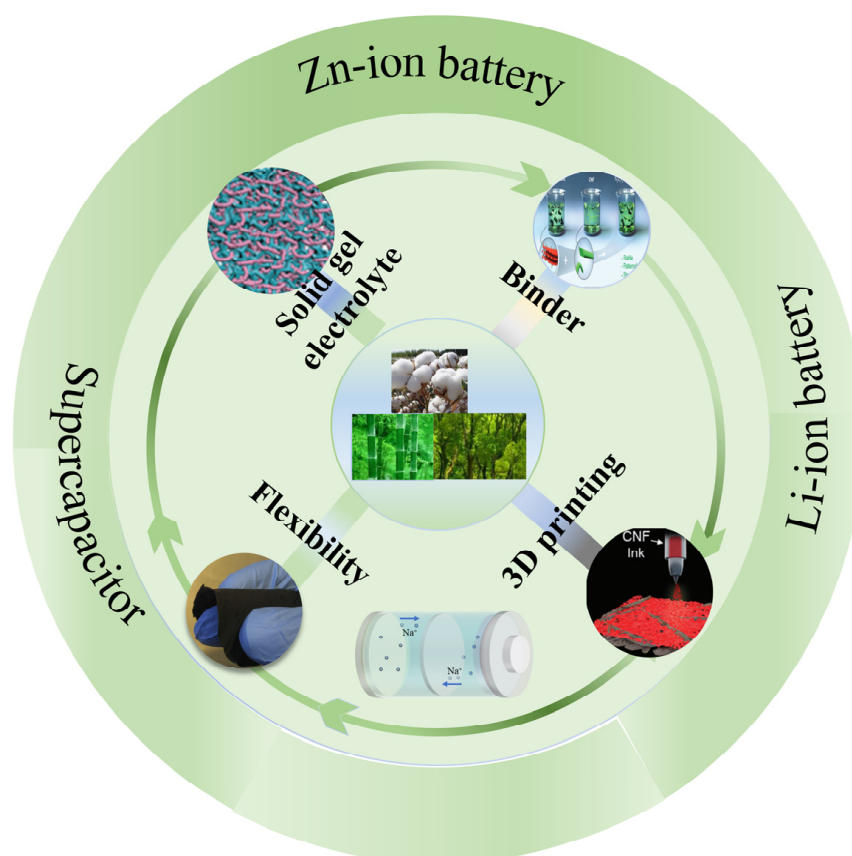


Figure 1. Schematic diagram showing the main topics of this review from cellulose resources, nanocellulose fabrication, and functional design to energy storage devices.

The advancement of CNF-based energy devices holds the potential for sustainable and environmentally friendly energy solutions. Recently, several reviews have compiled the utilization of nanocellulose and its derived materials in supercapacitors, lithium-ion batteries (LIBs), and various energy conversion devices. In this review, we present a comprehensive pathway towards CNF-based energy devices using cellulose as a starting point. We propose that a desirable strategy to achieve our goals involves a combination of recycling, biomass utilization, and carbon capture and utilization for printing batteries. However, limited literature exists that summarizes the use of CNFs in electrolytes, electrodes, binders, and particularly as substrates for 3D printing inks. Thus, this review aims to provide an

overview of the current state of research on biomass-derived CNFs and their fabrication methods, properties, and potential applications in energy storage and transformation.

2. Preparation and Properties of Nanocellulose

CNFs are polyoses that exist as linear chains composed of repeating anhydro-D-glucose units linked by β -1,4-glycosidic bonds. Figure 2 illustrates the schematic representation of CNFs derived from plants. The diverse properties of CNFs stem from their plentiful surface hydroxyl functional groups and high aspect ratio, which facilitate both intra- and inter-molecular interactions. These characteristics contribute to the unique and versatile nature of CNFs.

2.1. The Fabrication of CNFs

In this section, we provide a review of the preparation methods for biomass-derived CNFs. In the 1980s, Turbak and his colleagues at ITT Rayonier pioneered the creation of CNFs through nanofibrillation [1]. The nanofibrillation process involves subjecting wood cellulose pulps to physical techniques such as high-pressure homogenizers, grinders, and high-intensity ultrasonicators in aqueous media to obtain CNFs. Another study by Abe et al. demonstrated the fabrication of nanofibrillated cellulose (NFC) with a consistently uniform width of approximately 15–20 nm using mature bamboo [16]. These methods highlight the progress made in achieving the efficient and controlled production of CNFs from various biomass sources. Moreover, enzymatic hydrolysis along with mechanical nanofibrillation represents another approach for generating CNFs. Pääkkö et al. successfully fabricated CNFs with two distinct aspects: one with a lateral dimension of 5–6 nm and the other with lateral nanofiber bundle dimensions of approximately 10–20 nm [17]. However, despite the various mechanical nanofibrillation methods available to produce high-aspect-ratio CNFs, the formation of aggregates remains a challenge that needs to be addressed. To enhance the nanofibrillation process, Isogai et al. made significant advancements by introducing the TEMPO (2,2,6,6-tetramethylpiperidine-1-oxyl radical)-mediated oxidation method. This pioneering technique facilitated the production of uniformly dispersed individualized CNFs [18]. Furthermore, Okita et al. demonstrated that the TEMPO-mediated oxidation procedure effectively exposed all the C6 primary hydroxyls on the surfaces of cellulose microfibrils, predominantly transforming them into sodium carboxylate groups [19].

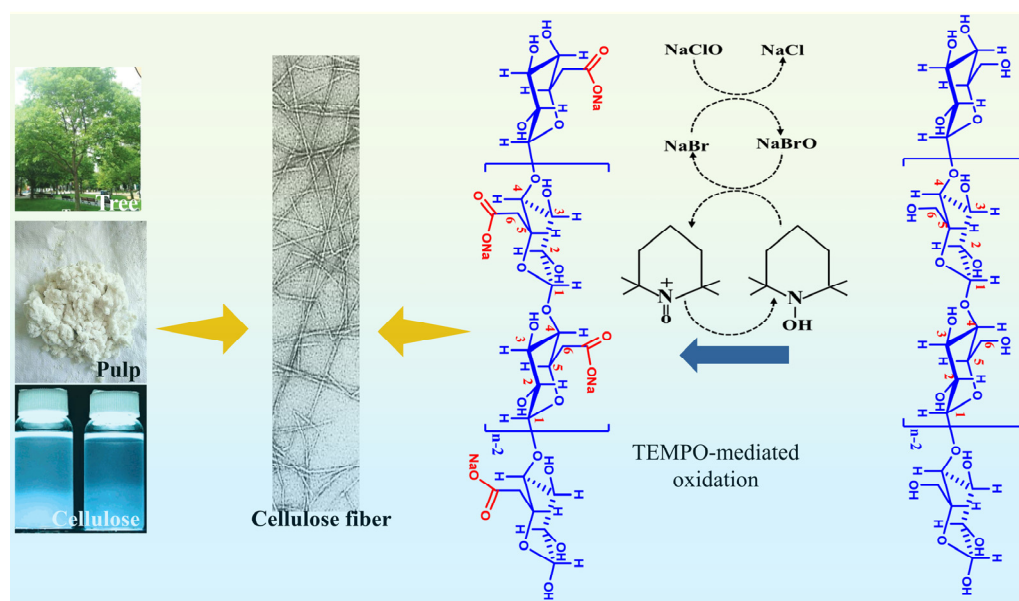


Figure 2. The sample and fabrication of the CNF-based TEMPO method [19]. Copyright (2019) Wiley.

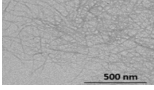
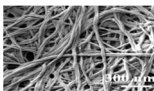
2.2. Production Methods of Biomass-Derived Nanofibers

Nanofibrillated cellulose (NFC), cellulose nanocrystals (CNC), and bacterial cellulose (BC) are widely utilized in the literature, offering diverse sources and synthesis methods that yield various structures and surface chemistry properties, as presented in Table 1. For instance, spherical cellulose nanoparticles have been developed from a range of cellulose derivatives, while ribbon-shaped cellulose nanofibers have been obtained through the electrospinning technique using cellulose-based precursors. This section focuses on the preparation of biomass-derived CNFs, which can be achieved through several methods, including physical, enzymatic, and chemical treatments.

The morphology of CNFs exhibits variations influenced by both the source of the biomass and the preparation method employed, resulting in significant disparities in fiber length, diameter, and crystallinity. Among the available resources, lignocellulosic fibers are widely preferred for CNF production. This choice is attributed to their abundant availability, cost-effectiveness, renewability, and ease of processing [20]. In addition to lignocellulosic fibers, non-lignin sources such as flax, sisal, and cotton, agricultural residues like rice straw, and certain non-lignocellulosic fibers have gained attention for CNF production [21–24]. These alternative sources offer advantages such as the easier extraction of non-lignocellulosic cellulose from the primary cell wall, requiring less time and energy. As a result, these materials hold promise as viable options for environmentally sustainable circular bioeconomies, enabling the production of CNFs with satisfactory properties at a low cost. The production of CNFs often involves three commonly employed mechanical methods: common refiners, ultrafine super grinders or micro grinders, and high-pressure homogenizers (HPHs) or high-pressure microfluidizers (HPMs). These mechanical approaches primarily rely on the grinding of cellulose, offering high efficiency and suitability for large-scale production [25–27]. Nevertheless, this method has certain limitations, such as the incomplete breakdown of cellulose fibers, equipment blockages, high energy consumption, potential damage to the crystal structure, and the requirement for repeated mechanical treatment to achieve high-quality CNFs. In contrast, enzymes offer an alternative approach by selectively cleaving internal hydrogen bonds at random amorphous sites, leading to the generation of new chain ends. This enzymatic action facilitates more precise and controlled fiber breakdown, enhancing the production of high-quality CNFs [28].

Enzyme pretreatment provides several notable benefits prior to the preparation process, such as decreased energy consumption and minimized equipment blockage during mechanical crushing. These advantages ultimately contribute to cost reduction and improved efficiency in CNF production [29]. Furthermore, enzyme pretreatment offers the added advantage of being more environmentally friendly compared to chemical methods. While enzymatic treatment may be relatively less efficient than chemical treatment, the chemical pretreatment of cellulose fibers continues to be widely used to reduce the mechanical energy needed for processing through HPHs and HPMs. This method involves converting the hydroxyl group (-OH) of cellulose fibers into a carboxyl group (COO-), resulting in the generation of repulsive forces within the fiber's internal structure. This modification facilitates easier fibrillation and improves the overall efficiency of the CNF production process [30]. This weakens the cellulose structure, making it easier to mechanically disintegrate the fibers [31]. Furthermore, 2,2,6,6-tetramethylpiperidine-1-oxyl (TEMPO)-mediated oxidation, discovered by Akira Isogai et al., is a prominent example of pretreatment for the production of CNFs [32]. This breakthrough was awarded the Wallenberg Award. By utilizing this technique, the energy requirement for producing one ton of CNFs is reduced from 30,000 kWh to 100–500 kWh, resulting in a more consistent CNF product [33–35]. Periodate-chlorite oxidation of carboxymethyl cellulose (CMC)-modified cellulose fibers is a common variation of this approach [36–39]. This nanofibrillated cellulose has the potential to be developed for energy storage applications.

Table 1. Source, morphology, structure, and fabrication of nanocellulose.

Type	Source	Morphology	Representative SEM/TEM Image	Surface Chemical Group	Fabrication Method	Reference
CNF	Wood	Thread-like aggregates		Hydroxyl carboxylate	TEMPO-mediated oxidation and stirring	[40]
CNC	Cotton	Rod-like particles		Hydroxyl	Sulfuric and hydrolysis	[41]
BC	Coconut milk	Thread-like aggregates forming hydrogels		Hydroxyl	Secreted by Acetobacter xylinum FF-88	[42]

3. CNFs as Binders in Energy Storage and Conversion

Adhesives are utilized in the production of batteries and supercapacitor electrodes to effectively bond the components, forming a uniform layer that securely attaches to the current collector [43]. Polyvinylidene fluoride (PVDF) is universally recognized as the predominant binder in both industrial and academic settings, owing to its exceptional capability to bind active materials together, resulting in the formation of high-quality electrode materials [44]. Renowned for its superior mechanical stability and controlled expansion properties, this semi-crystalline fluoropolymer, PVDF, excels in delivering exceptional electrode performance and seamless integration. Additionally, PVDF polymers inherit the renowned stability of fluoropolymers, complemented by excellent resistance to chemicals and oxidation. Nevertheless, their hydrophilicity is limited, and they demonstrate notable swelling characteristics when exposed to electrolytes. This makes them well suited for electrode applications with N-methyl-2-pyrrolidone (NMP) as a dispersant, specifically for cathodes like lithium nickel cobalt manganese oxide (NCM) [45]. While organic dispersants have conventionally been employed, they come with several disadvantages, including volatility, high toxicity, flammability, and explosiveness. It is worth mentioning that the drying process for electrode preparation requires additional heat and time due to the high boiling point of NMP. Prolonged drying not only increases energy consumption but also leads to the diffusion of PVDF to the surface [46]. Consequently, there is a growing interest in exploring water-based dispersants that offer enhanced environmental protection and safety, making them promising contenders for the next generation of electrode dispersants. Furthermore, it is worth highlighting the costliness of PVDF, underscoring the importance of developing affordable aqueous binders.

CNFs (carbon nanofibers) exhibit a remarkable water absorption capacity, allowing for the production of highly viscous suspensions even at low concentrations (<5 wt.%). In 2005, CMC (carboxymethyl cellulose) was first employed to facilitate the water treatment of graphite particles specifically for graphite anodes [47]. The efficacy of CMC as a dispersant for graphite particles in aqueous solutions has been well documented. This behavior can be attributed to the structure of the polymer, wherein the hydrophobic section of CMC adheres to the hydrophobic graphite surface. Simultaneously, the carboxyl groups present in the adsorbed CMC layer acquire an electric charge, thereby stabilizing the graphite surface in water [48].

CNF has emerged as a versatile material for the fabrication of flexible electrodes, following a preparation process akin to papermaking. A solution containing the active material, conductive agent, and binder is thoroughly blended, and the solvent is then eliminated through suction filtration. This process yields a self-supporting, flexible electrode. Tian et al. successfully crafted freestanding and flexible nanopapers from $Ti_3C_2T_x$ /CNF dispersions, employing the vacuum filtration method [49]. The composites demonstrate analogous layered structures to the original MXene films (Figure 3a–c). Furthermore, Lei-

Jonmarck et al. [50] employed a papermaking process to fabricate a flexible cathode by utilizing a lithium iron phosphate (LiFePO_4) cathode and CNFs as a binder (Figure 3d). The electrode produced via the papermaking process exhibits flexibility, making it well suited for applications in flexible batteries. (Figure 3e,f). Cornell et al. [51] conducted a comprehensive investigation to assess the influence of charge density and degree of homogenization of CNFs on the properties of CNF electrodes.

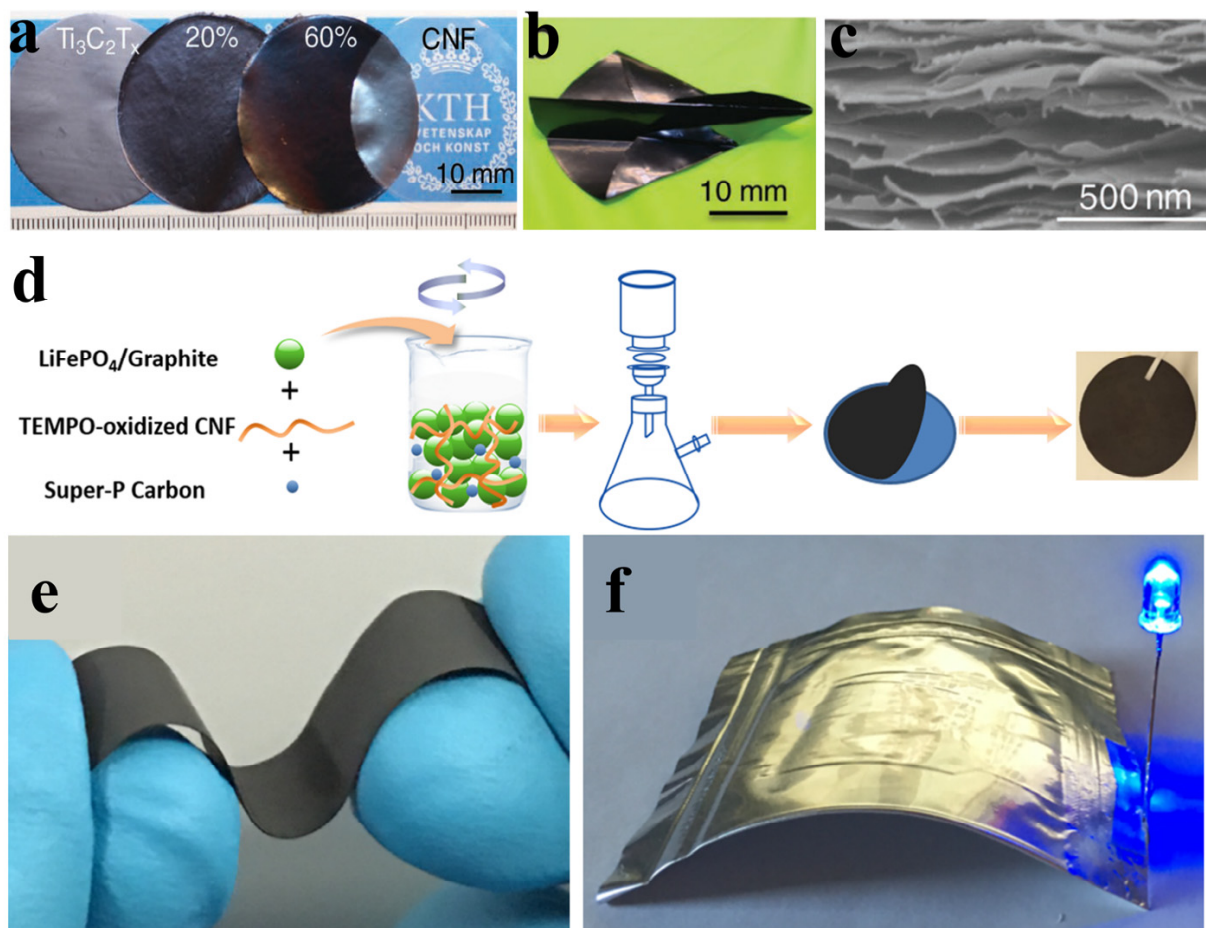


Figure 3. (a) Morphology characterization of $\text{Ti}_3\text{C}_2\text{T}_x$ MXene/CNF nanopapers. (b) Photography of nanopaper folded into the shape of an airplane to show the mechanical flexibility. (c) SEM cross-sectional images (bottom) of $\text{Ti}_3\text{C}_2\text{T}_x$ /CNF [49]. Copyright (2019) Wiley. (d) Schematic illustration of the water-based paper-making process for flexible electrodes. (e) Photograph of a positive electrode made from flexible paper. (f) A cell that has been bent [50]. Copyright (2017) American Chemical Society.

The strength of CNF bonding can be influenced by several factors, such as pretreatment process, chemical modification, fiberization degree, surface charge, concentration, and fiber aspect ratio. Notably, CNFs with a higher surface charge exhibit enhanced electrostatic repulsion, leading to improved homogenization efficiency and a narrower length distribution. The findings demonstrate that a higher charge density in CNFs confers advantages in enhancing both the mechanical properties and electrochemical performance. In the scenario of CNFs with a lower charge density, augmenting the degree of homogenization positively affects the electrode's mechanical and electrochemical performance. However, for electrodes utilizing CNFs with a higher charge density, an increased degree of homogenization can adversely impact the outcomes. Guo et al. [52] introduced a simple yet effective method for bonding binders and electrolytes, resulting in a remarkable improvement in the cycle stability of high-capacity anodes utilizing potassium ions. By employing a combination

of chemically interconnected carboxymethylcellulose and polyacrylic acid (CMC + PAA) binders along with compatible electrolytes, the electrodes' durability and consistency can be significantly enhanced.

Supercapacitor and Li-ion battery electrodes are typically fabricated by combining active materials with polymer binders such as polyvinylidene fluoride (PVDF) and polytetrafluoroethylene (PTFE) [53,54]. However, conventional binders, despite constituting more than 5% of the electrodes' total mass, often result in the surface coating of carbon materials and pore blockage [55]. Notably, Lacey et al. [56] conducted research revealing that the integration of PVDF with carbon materials in an NMP solution can lead to a significant loss of porosity. Furthermore, binders containing fluorine groups exhibit superhydrophobic properties, leading to water repellency. This hydrophobic nature, coupled with their tendency to fill pores, hinders the accessibility of electrolyte ions to the active material. Consequently, this insulating effect between the active material and electrolyte ions negatively impacts device energy density, resulting in reduced performance. Moreover, it is worth noting that PVDF adhesive exhibits instability in strongly alkaline environments [57]. In contrast, CNFs possess a plethora of hydrophilic groups, and their one-dimensional structure has a minimal impact on the pore structure of carbon-based materials. Nonetheless, bonding CNFs with specific active materials, particularly those with low strength, can present challenges. Ni et al. [58] presented findings demonstrating that the utilization of CNF (cellulose nanofiber) adhesive effectively maintains the microporosity of biochar charcoal while enhancing its moisture retention. Figure 4a illustrates the schematic diagram of the electrode preparation process, where CNF serves as a binder to bind the activated biochar, consequently preserving a significant number of micropores, leading to improved ion-accessibility. Moreover, the SEM analysis reveals that the CNF binder forms a fibrous network, uniformly enveloping the biochar particles, as depicted in Figure 4b. To demonstrate the wetting capability of CNF- and PVDF-based electrodes, water contact angles were measured and presented in Figure 4c. The results indicate that the water droplet dispersed within a mere 0.02 s on CNF-coated nickel foam, whereas the PVDF-coated nickel foam showed no change even after 5 min. The results demonstrate the exceptional wetting property of CNF binder networks. The inherent hydrophilic nature of CNFs enhances the accessibility of electrolyte ions to the active material, leading to a substantial reduction in the electrode's bulk electrolyte resistance and an increase in its capacitance. Specifically, the replacement of PVDF with CNF adhesive decreased the internal resistance of the electrode from 1.5 Ω to 0.76 Ω . (Figure 4d,e). The BN-AC/CNF system exhibited an enhanced capacitance of 268.4 F g⁻¹, demonstrating remarkable durability with a capacitance maintenance rate of 96.2% even after 10,000 cycles (Figure 4f,g). The observed rate was notably higher compared to that of BN-AC/PVDF (187.9 F g⁻¹, 96.2%). Notably, even at high power densities, the BN-AC/CNF electrode outperformed the PVDF adhesive electrode in terms of energy density, showcasing a substantial improvement.

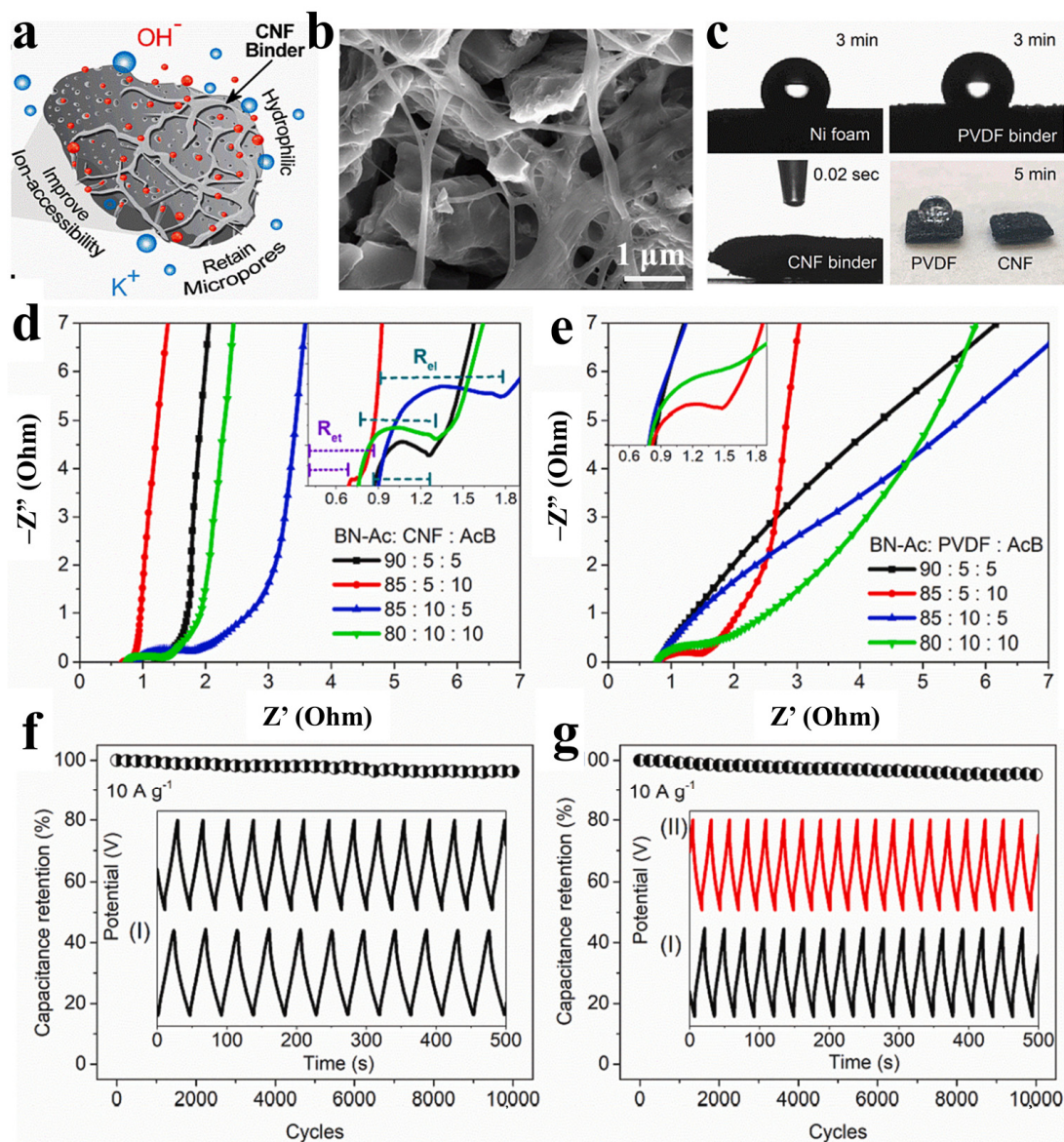


Figure 4. (a,b) The schematic diagram (a) and SEM (b) of the prepared biochar/CNF-binder-based electrode; (c) water contact angle on various electrodes. X Nyquist plots (d,e) and cycling durability after 10,000 cycles at 10 A g⁻¹ (f,g) are presented for BN-Ac electrodes bound with NF- and PVDF-binders [58]. Copyright (2023) Elsevier.

4. The Application of CNFs in Gel Electrolyte

Flexible devices distinguish themselves from conventional power setups through the utilization of electrode materials and electrolytes that possess exceptional flexibility. The electrolytes, in particular, demonstrate remarkable pliability, enabling the creation of devices with diverse shapes, lightweight construction, high deformability, and compact size. This versatility renders them highly suitable for flexible and wearable electronic devices. Consequently, the electrolyte requirements encompass several crucial aspects, including outstanding ionic conductivity, efficient electrode–electrolyte contact, minimal resistance at the electrode–electrolyte interface, flexibility, and robust stability, even under high-temperature conditions.

Cellulose-based gel electrolytes have limitations in their suitability for lithium-ion batteries. The main challenge arises from the difficulty in achieving membrane formation, coupled with their inherently brittle nature and lack of conducting ionic properties [59,60]. Consequently, the films produced only serve as separators in LIBs [13]. Significant ad-

vancements are required to enhance the performance of cellulose-based gel electrolytes for them to become a viable option in lithium-ion batteries. Addressing this need, Zhang et al. developed a flexible all-solid-state electrolyte that incorporates brush-like cellulose [61]. Through the in vivo controllable polymerization, the ion-conducting segment was grafted onto a cellulose-based macroinitiator, giving rise to a highly stretchable all-solid-state electrolyte known as CSSPE (Figure 5a). Notably, CSSPE showcases an impressive ionic conductivity of $8.00 \times 10^{-5} \text{ S cm}^{-1}$ at room temperature. When applied in a $\text{LiFePO}_4/\text{Li}$ battery, CSSPE exhibits exceptional long-cycle durability and outstanding rate capacity. To showcase the potential of CNF-based electrolyte in flexible wearable devices, Figure 5b illustrates the schematic diagram of the gel MSC preparation. Moreover, when two MSCs are connected in series, it results in twice the operating voltage compared to a single MSC. Similarly, connecting them in parallel yields approximately twice the current and discharge time compared to a single MSC. These findings highlight the consistent performance of the CNF-based gel. Regardless of the curved state of the MSC, it can effectively power a digital watch for an extended period (Figure 5d). Importantly, the MSC retains its flexibility and integrity even after undergoing electrochemical testing, thereby demonstrating its robust application characteristics.

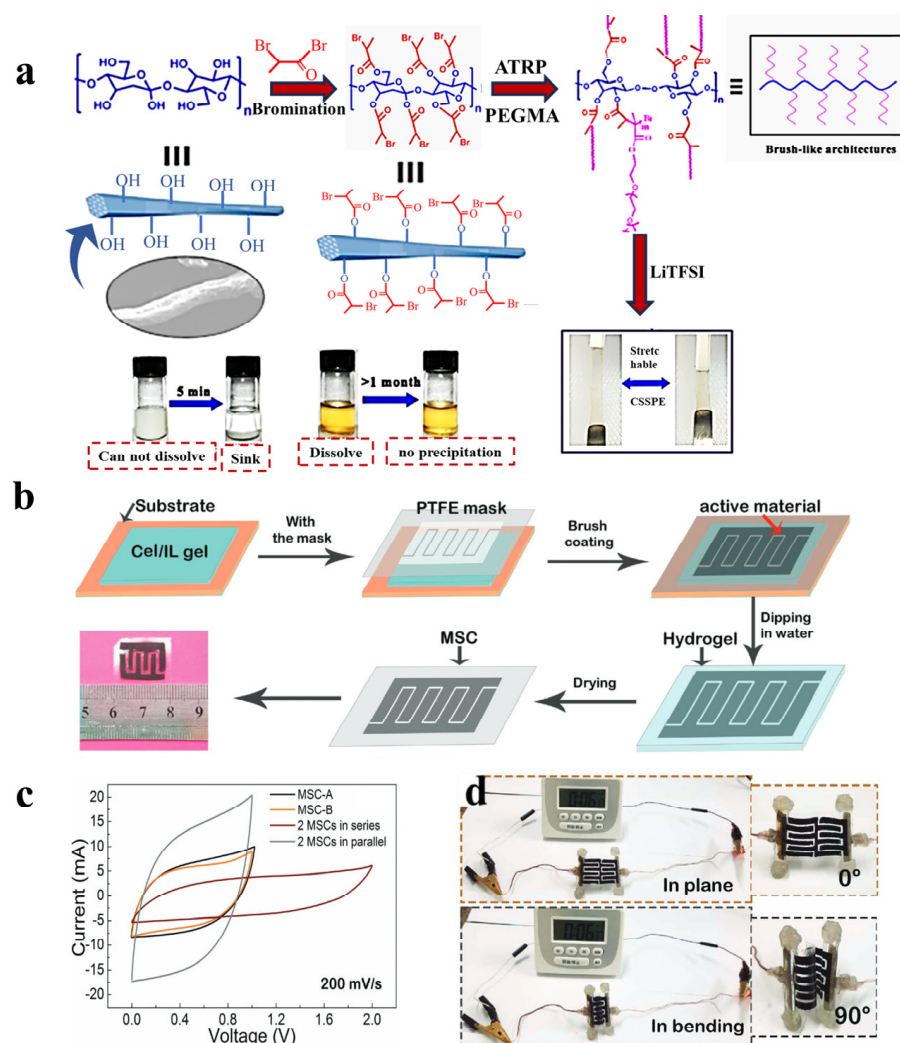


Figure 5. (a) The synthetic route used to prepare the cellulose-based polymer with brush-like architectures, referred to as CSSPE. (b) Schematic diagram of the CNF-gel-membrane-based series MSCs. (c) CV curves of two MSCs in series connection and in parallel connection. (d) Optical images of a digital watch operated by the mCel-membrane-based energy storage system [61]. Copyright (2020) American Chemical Society.

The polymer network structure of the gel electrolyte facilitates the effective entrapment of water molecules, leading to a remarkable balance between high ionic conductivity comparable to liquid electrolytes and prevention of water evaporation. This advantageous characteristic makes the gel electrolyte highly versatile and suitable for various applications, including zinc batteries, supercapacitors, and more. Gel electrolytes commonly utilize polymers such as polyvinyl alcohol (PVA) and sodium carboxymethylcellulose (CMC) [62,63]. Among them, PVA-based gel electrolytes are widely preferred due to the hydrogen bonds formed between PVA segments and water molecules, which contribute to enhanced viscosity within the gel electrolyte system [64]. The increased viscosity of PVA-based gel electrolytes plays a crucial role in enhancing the electrode-electrolyte interface, facilitating improved contact between the electrolyte and electrode material. On the other hand, CMC is another commonly used biomaterial in gel electrolyte formulation. However, the strong adhesion properties of CMC can lead to the complete coating of the electrode surface by the CMC-based gel electrolyte [65]. Wang et al. [66] demonstrated the fabrication of a noteworthy paper-based all-solid-state supercapacitor using CMC as the solid electrolyte. The negative charge of cellulose fibers in water, attributed to the uronic acid groups and polar hydroxyl, facilitates the successful adsorption of $[\text{Ag}(\text{NH}_3)_2]^+$ onto the cellulose surface through electrostatic interaction, as depicted in Figure 6a–c. Subsequently, a conductive Ag-Cell/RGO-Cell paper was obtained through a reduction and drying process, as shown in Figure 6d. To explore its practical application, the Ag-Cell/RGO-Cell paper was assembled into a symmetric fully cellulose based all-solid-state supercapacitor, and its electrochemical performance was evaluated, as presented in Figure 6e. The all-solid-state supercapacitor exhibited exceptional performance with a low internal resistance, achieving a capacity of 222.5 F g^{-1} at a current density of 1 A g^{-1} . Even at a higher current density of 10 A g^{-1} , it maintained a mass-specific capacitance of 150 F g^{-1} , retaining 67.4% of its initial capacity. Moreover, when fully charged, the series-connected supercapacitors were able to power a red-light-emitting diode, as illustrated in Figure 6g. These results highlight the potential of cellulose-based all-solid-state supercapacitor paper for various wearable electronic devices.

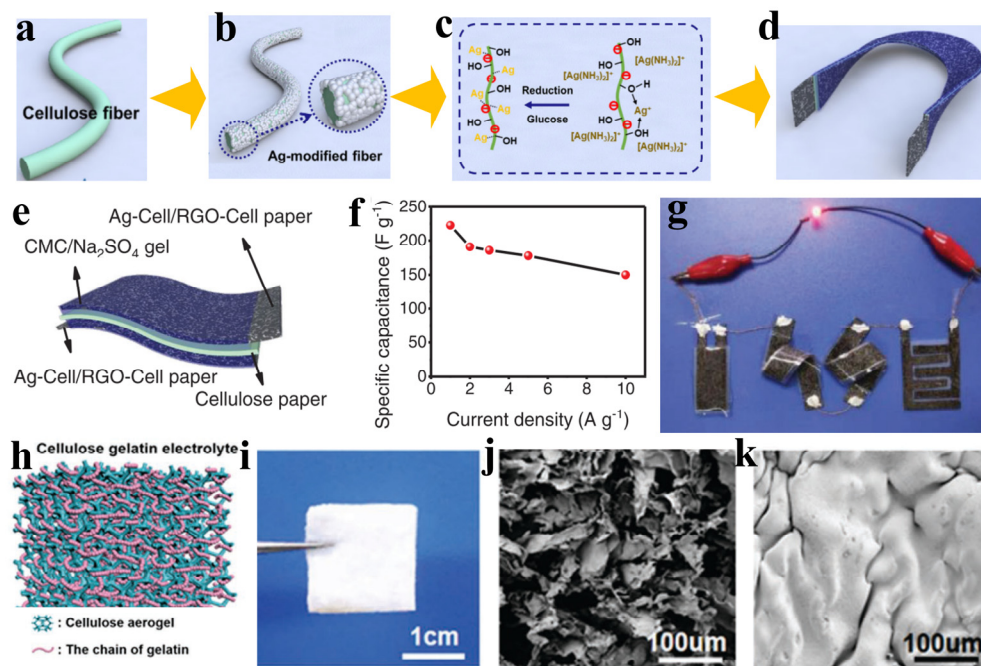


Figure 6. (a–e) Schematic structure of the assembled supercapacitor device, (f) specific capacitance at different current densities, (g) the digital photographs of a red LED lit by the various supercapacitor devices in series, (h) the structure and morphologies of the CAG electrolyte, (i,j) optical and SEM images of the CA framework, (k) SEM images of the CAG electrolyte film [66]. Copyright (2021) Wiley.

Zinc-ion batteries (ZIBs) offer a promising solution to various challenges due to their abundance and superior safety compared to lithium and other metals [67]. Kong et al. [68] presented a degradable ZIBs, which employed a biodegradable cellulose-aerogel-gelatin (CAG) electrolyte. The battery architecture consisted of a silk protein film, an in situ evaporated gold film, a screen-printed zinc film, and MnO_2/rGO composites, serving as the encapsulation layer, collector, cathode, and anode materials, respectively. The fabrication process entailed freeze drying a 3D aerogel framework, which was subsequently infused with a mixture of pristine gelatin chains, ZnSO_4 , and MnSO_4 . The resulting crosslinked porous hydrogels exhibited remarkable mechanical properties and flexibility. Figure 6h provides insight into the structure and morphologies of the CAG electrolyte. The CA framework appears as a white, tile-like film with robust mechanical strength (Figure 6i). Scanning electron microscopy (SEM) images of the CA framework (Figure 6j) reveal a highly porous 3D morphology. The image (Figure 6k) demonstrates the successful grafting of gelatin chains onto the CA framework, resulting in the formation of a CAG film.

Recently, Hu et al. [69] demonstrated a biopolymer shell-chitosan-zinc gel electrolyte for high-rate and long-life zinc metal batteries. The chitosan-Zn membrane exhibited a hierarchically porous structure (Figure 7a), featuring large pores measuring up to 5 mm in diameter (Figure 7b,c). It facilitates the rapid and even conduction of Zn^{2+} ions, while simultaneously restricting ion flux perpendicular to the Zn anode surface. This results in the formation of tightly packed parallel Zn platelets on the anode (Figure 7d). This deposition morphology effectively reduces the interface area between the electrolyte and Zn, minimizing interfacial side reactions. These improvements significantly enhance the cycling reversibility and lifespan of the Zn anode. In contrast, the aqueous electrolyte, despite having high Zn^{2+} ionic conductivity, allows Zn^{2+} ions to diffuse from all directions due to its ubiquity. Consequently, in the liquid electrolyte, Zn metal plating tends to form perpendicular-oriented platelets (Figure 7e) along the shortest diffusion path, which adversely affects the reversibility and stability of the anode. Furthermore, the coulombic efficiency of $\text{Zn} \parallel \text{Cu}$ cells, which serves as an indicator of the Zn anode's performance, was evaluated using different electrolytes. Remarkably, even under a high current density of 50 mA cm^{-2} , the chitosan-Zn electrolyte demonstrated the capability to sustain the stable cycling of the Zn-metal anode for 1000 cycles. The anode exhibited a capacity of 10 mAh cm^{-2} and a depth of discharge of 17.1% without experiencing significant voltage fluctuations (Figure 7f). Conversely, when using the aqueous electrolyte, the cell exhibited irreversible voltage increase and eventually failed at the 350th cycle.

To further optimize the application scope of biomass-based electrolytes in zinc-ion batteries, a hydrogel electrolyte has been developed, characterized by a denser structure that helps suppress the growth of zinc dendrites. In this regard, Hu et al. [70] showcased a nanocellulose-carboxymethyl-cellulose (CMC) electrolyte. This electrolyte exhibits high ionic conductivity, mechanical strength, and low free water content, enabling a high-rate and long cycling life for aqueous ZIBs, as shown in Figure 7g–i. To evaluate the performance of the cellulose-5 wt.% CMC electrolyte in a full cell, the researchers utilized the conventional $\text{Zn} \parallel \text{MnO}_2$ as electrodes. It exhibited exceptional rate performance, as evidenced by both the discharge profile (Figure 7j) and cycling performance (Figure 7k). The cellulose-CMC electrolyte offers significant advantages, such as its easy accessibility and low-cost nature abundance. These qualities make it highly promising for utilization in Zn-ion batteries, thereby paving the way for grid-scale energy storage solutions for renewable energy sources.

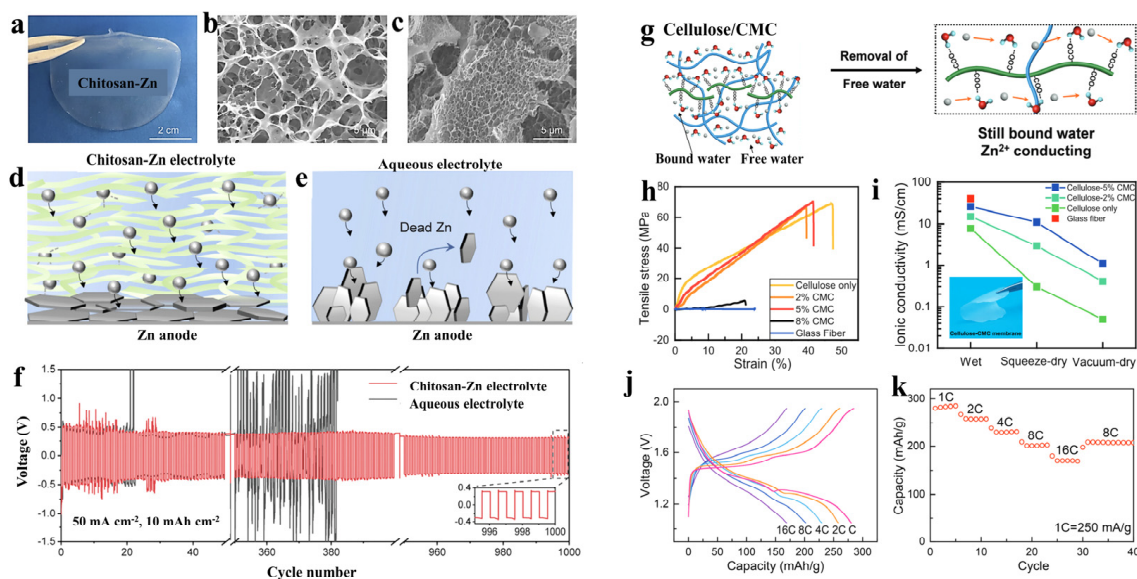


Figure 7. Photographs (a) and SEM images depicting the (b) surface and (c) cross-sectional morphology of the porous chitosan-Zn membrane. Schematic diagrams illustrating Zn plating on the Zn anode utilizing various electrolytes, including (d) chitosan-Zn and (e) aqueous electrolyte. (f) the galvanostatic Zn plating/stripping was performed in a Zn || Zn symmetric cell cycled with chitosan-Zn and aqueous electrolytes at a current density of 50 mA cm⁻² and a capacity of 10 mAh cm⁻² [69]. Copyright (2022) Cell Press. Utilizing cellulose-CMC electrolyte for aqueous zinc-ion Batteries (g). Tensile testing of various NaOH-treated cellulose-CMC membranes compared to a glass fiber separator as a control (h). Measurement of ionic conductivity in a wet glass fiber separator, as well as different cellulose-CMC membranes under various drying conditions. The inset showcases a digital image of the cellulose-CMC electrolyte (i). The rate performance of discharge profile (j) and cycling performance (k) [70]. Copyright (2023) Wiley.

5. The Application of CNFs in 3D Printing

3D printing machines utilize a streamlined process to produce high-resolution three-dimensional objects, offering exceptional efficiency and versatility. This technology enables the rapid creation of various 3D structural prototypes [71,72]. Cellulose 3D printing extends beyond hydrogel 3D printing [6] and finds applications in diverse domains such as plastics [73], smart paper [74], biomedicine [75], electronic equipment [76], sensors [77], and other industries. Qiu et al. [78] demonstrated the use of carboxymethyl cellulose-lithium as a positive electrode binder for lithium-ion batteries, leading to improved electrochemical performance of LFPO and remarkable stability. In another application, cellulose is employed in battery technology through the 3D printing of nanocellulose, enabling the fabrication of high-performance lithium metal batteries. The nanocellulose gel exhibits exceptional shear-thinning properties, facilitating the printing of LFPO electrodes and stable lithium scaffolds. The high aspect ratio of nanocellulose (10–50 nm wide by 500–2000 nm long) and its anionic surface charge play a significant role in the shear-thinning behavior. These properties contribute to the formation of robust hydrogels at low concentrations, driven by anion repulsion and hydrogen bonding, without the need for additives. When incorporated into cellulose nanofiber hydrogels, the ink exhibited shear-thinning behavior at a shear rate of 10 s⁻¹. The porous structure of the nanofibers enhances ion accessibility and reduces the local current density of the lithium anode. Cellulose nanofibers are widely used as a matrix material due to their ability to increase viscosity and exhibit thixotropic rheology. Kim et al. [79] demonstrated the utilization of carboxymethyl cellulose (CMC) as a framework and silver nanowires (AgNWs) as a conductive agent for the fabrication of 3D conductors (Figure 8a–c). The voltage profile of the 3D printed battery during the charging process is illustrated in Figure 7d, showing an increase in voltage to approximately 1.2 V after 85 min and 1.8 V after 275 min. In another study, Zhu et al. employed

cellulose-nanofiber-based inks in the 3D printing method to enhance the electrochemical performance and stability of lithium metal batteries (LMBs). As a matter of fact, the rheological properties of the ink are crucial for successful printing. Figure 8d displays images of the prepared white CNF gel, CNF ink, CNF/LFP ink, and the aqueous dispersion of LFP stored in bottles, with all CNF-containing inks exhibiting high viscosity and adhering firmly to the bottom of the bottle. Figure 8e demonstrates that all three samples exhibit non-Newtonian fluids with shear-thinning properties, which greatly contribute to their exceptional printability. Moreover, to highlight the remarkable printability, the CNF scaffold consisting of 21 layers maintained its desired structure even after water removal and carbonization, as depicted in Figure 8f. Figure 8g provides an enlarged photo of the as-printed CNF scaffold surface, revealing its porous and layer-by-layer architectures. The presence of large pores can be attributed to the absence of water during the freeze-drying process. Furthermore, Figure 8h presents the charge and discharge profiles of the cell with the printed c-CNF/LFP cathode at 0.2 C, demonstrating its stability. During the initial two cycles, notable charge and discharge capacities of 167 and 140 mA h g⁻¹ were achieved, respectively. Figure 8i displays the charge/discharge curves of the printed full cell, illustrating its rate performance. The discharge capacities at various discharge rates were as follows: 137, 131, 120, 107, 93, and 80 mA h g⁻¹ at discharge rates of 0.2, 0.5, 1, 2, 5, and 10 C, respectively.

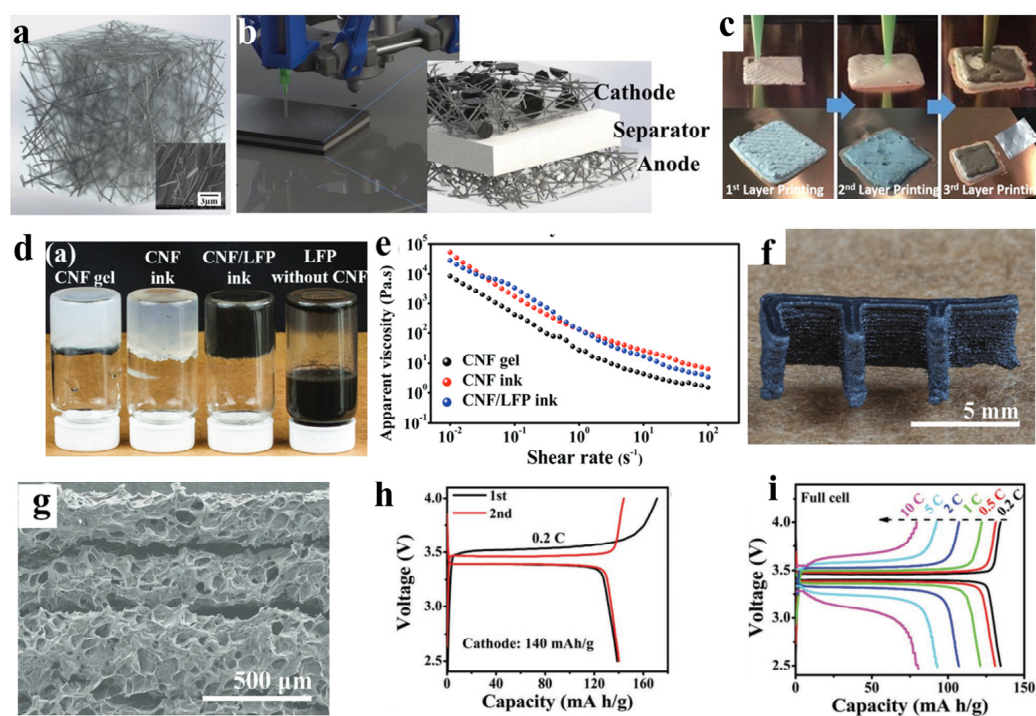


Figure 8. Schematic designs of cellulose composites and 3D printing of battery composites. (a) Computer-aided design (CAD) model of AgNWs/CMC 3D Conductor, (b) CAD representation of three-layered 3D-printed battery, (c) images of the 3D printing process of the 3D-printed battery, (d) pristine CNF gel, CNF ink, CNF/LFP ink, and LFP dispersion stored in inverted vials to show viscosity, (e) apparent viscosity as a function of shear rate for pristine CNF gel, CNF ink, and CNF/LFP ink, (f) 3D-printed c-CNF scaffold after carbonization, (g) surface of printed c-CNF, (h) charge and discharge profiles of the cell with c-CNF/LFP cathode at 0.2 C, (i) voltage profiles at various rates from 0.2 to 10 C [79]. Copyright (2017) Nature.

To enhance the 3D printing capabilities of MXene-based inks with low MXene loading, Mei et al. [80] developed controllable cellulose nanofibers (CNFs) through a TEMPO-mediated oxidation process. Furthermore, CNFs serve as an intercalation agent, preventing the aggregation of MXene nanosheets and facilitating the formation of a hierarchical porous

structure. This unique structure contributes to exceptional capacitance and rate performance. A series of sequential steps involving hot water treatment, NaClO_2 and NaOH treatments, TEMPO-mediated oxidation, and ultrasonication were employed to isolate cellulose nanofibers (CNFs) from palm oil fibers. The resulting CNFs were then utilized to fabricate MXene/CNF ink, and its rheological properties were evaluated. Subsequently, a solid-state symmetric supercapacitor was constructed using two 3D-printed pectinate electrodes (Figure 9b–d). Two types of inks, with and without CNF, were prepared (Figure 9e), demonstrating the suitable viscosity attributed to the incorporation of CNF. Upon extrusion, the pure MXene ink with low viscosity exhibited droplet formation (Figure 9e, top), resulting in discontinuous flow. However, the MXene/CNF10 ink (Figure 9e, bottom) displayed a uniform and continuous filament due to its enhanced homogeneity and improved rheological properties. The cyclic voltammetry (CV) curve (Figure 9f) demonstrated a nearly symmetrical and nonlinear triangle, indicating the high reversibility of the charge/discharge process and the pseudocapacitive nature of MXene. Moreover, the galvanostatic charge–discharge (GCD) curves (Figure 9g) showcased the excellent rate performance of MXene, with a retention rate of approximately 70% at 20 mA cm^{-2} . These findings, as depicted in Figure 9, highlight the suitability of MXene for 3D-printed electrodes, showcasing exceptional rate performance and efficient surface utilization.

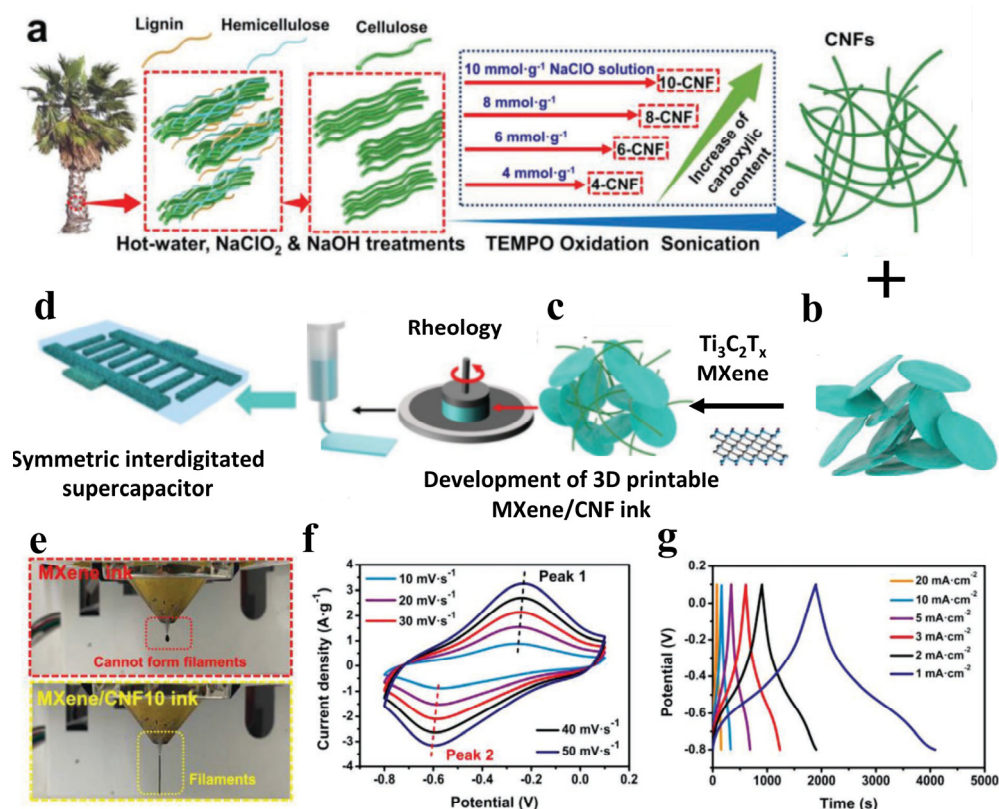


Figure 9. (a) Extraction of 1D CNFs from palm tree trunk oil via a series of steps including hot water, NaClO_2 and NaOH treatments, TEMPO oxidation, and sonication. (b,c) Characterization of MXene (Ti_3C_2) and MXene/CNF ink, and evaluation of their rheological properties. (d) Fabrication of a solid-state symmetrical supercapacitor using two 3D-printed pectinate electrodes. (e) Digital appearance of MXene and MXene/CNF10 inks during extrusion, and electrochemical performance of 3D-printed MXene/CNF10. (f) CV profiles. (g) GCD profile [80]. Copyright (2022) Wiley.

In conclusion, 3D printing holds immense promise in diverse applications and offers exciting opportunities for leveraging the capabilities of cellulosic materials. Particularly, the use of cellulose in 3D printing enables the fabrication of energy storage and conversion materials with customizable layered structures and specific functionalities. Although

significant progress has been made in researching cellulose-based 3D printing, further investigation into this fascinating field is warranted to unlock its full potential.

6. Conclusions

Cellulose nanofibers (CNFs) are an innovative material known for their renewable nature and exceptional mechanical properties. While CNFs have found commercial applications, their potential in the energy sector has been limited due to high production costs and stringent performance requirements. This review article is the first of its kind to explore the diverse applications of CNFs as binders, gel electrolytes, and in 3D printing. By addressing the existing challenges and providing a comprehensive summary of the relevant literature, this review aims to facilitate the broader utilization of CNFs in energy storage and conversion, offering insights into their promising prospects in this field.

Due to its nanoscale dimensions, high specific surface area, significant relative crystallinity, reactive surfaces rich in hydroxyl groups, entangled web-like structures, and favorable mechanical and thermal properties, nanocellulose holds great potential for various applications in electrochemical energy storage. These include: (1) The construction of self-standing electrodes or separators with high strength. (2) Integration with other electrochemically active materials. (3) The development of flexible substrates/scaffolds for flexible devices. (4) The design of multifunctional separators. (5) The synthesis of carbon-based porous materials and carbon hybrid materials. (6) The fabrication of diverse materials and various structures through 3D printing.

Nanocellulose-derived materials offer distinct advantages for a wide range of electrochemical energy storage applications, such as supercapacitors, lithium-ion batteries (LIBs), and Zn-ion batteries (ZIBs). Despite the successful development of nanocellulose-based advanced materials/devices for high-performance energy storage, there are still certain challenges that need to be addressed in the future, such as large-scale fabrication, surface/interface engineering, flexibility, new materials, and new applications.

Author Contributions: Writing—original draft preparation, R.L. and B.Z.; writing—review and editing, L.C. and H.F.; visualization, Q.L.; project administration, D.T.; funding acquisition, Y.L. and L.Y. All authors have read and agreed to the published version of the manuscript.

Funding: This work was financially supported by the Anhui Higher Education Institutions of China (No. 2022AH051582) and Huainan Normal University (No. 2022XJYB042) and the Opening Foundation of State Key Laboratory of Cognitive Intelligence, iFLYTEK (COGOS-2023HE02), the Doctor of Suzhou University Scientific Research Foundation Project (No. 2020BS014), the platform of Suzhou University (No. 2021XJPT16), and the Anhui Key Laboratory of low temperature Co-fired Materials (No. 2022LCA04).

Data Availability Statement: MDPI Research Data Policies at <https://www.mdpi.com/ethics> (accessed on 25 June 2023).

Acknowledgments: All individuals included in this section have consented to the acknowledgement.

Conflicts of Interest: The authors declare no conflict of interest.

References

1. Omer, A.M. Energy, environment and sustainable development. *Renew. Sustain. Energy Rev.* **2008**, *12*, 2265–2300. [[CrossRef](#)]
2. Ou, Z.; An, Z.; Ma, Z.; Li, N.; Han, Y.; Yang, G.; Jiang, Q.; Chen, Q.; Chu, W.; Wang, S.; et al. 3D Porous Graphene-like Carbons Encaged Single-Atom-Based Pt for Ultralow Loading and High-Performance Fuel Cells. *ACS Catal.* **2023**, *13*, 1856–1862. [[CrossRef](#)]
3. Tang, K.; Hu, H.; Xiong, Y.; Chen, L.; Zhang, J.; Yuan, C.; Wu, M. Hydrophobization Engineering of the Air-Cathode Catalyst for Improved Oxygen Diffusion towards Efficient Zinc-Air Batteries. *Angew. Chem. Int. Ed. Engl.* **2022**, *61*, e202202671. [[CrossRef](#)] [[PubMed](#)]
4. He, X.; Zhang, Y.; Wang, J.; Li, J.; Yu, L.; Zhou, F.; Li, J.; Shen, X.; Wang, X.; Wang, S.; et al. Biomass-Derived Fe₂N@NCNTs from Bioaccumulation as an Efficient Electrocatalyst for Oxygen Reduction and Zn-Air Battery. *ACS Sustain. Chem. Eng.* **2022**, *10*, 9105–9112. [[CrossRef](#)]

5. Yu, L.; Li, W.; Wei, C.; Yang, Q.; Shao, Y.; Sun, J. 3D Printing of NiCoP/Ti₃C₂ MXene Architectures for Energy Storage Devices with High Areal and Volumetric Energy Density. *Nanomicro Lett.* **2020**, *12*, 143. [[CrossRef](#)]
6. Lawson, S.; Alwakwak, A.A.; Rownaghi, A.A.; Rezaei, F. Gel-Print-Grow: A New Way of 3D Printing Metal-Organic Frameworks. *ACS Appl. Mater. Interfaces* **2020**, *12*, 56108–56117. [[CrossRef](#)]
7. Jin, H.; Li, J.; Yuan, Y.; Wang, J.; Lu, J.; Wang, S. Recent Progress in Biomass-Derived Electrode Materials for High Volumetric Performance Supercapacitors. *Adv. Energy Mater.* **2018**, *8*, 1801007. [[CrossRef](#)]
8. Kamel, S.; Ali, N.; Jahangir, K.; Shah, S.M.; El-Gendy, A.A. Pharmaceutical significance of cellulose: A review. *Express Polym. Lett.* **2008**, *2*, 758–778. [[CrossRef](#)]
9. Seddiqi, H.; Oliaei, E.; Honarkar, H.; Jin, J.; Geonzon, L.C.; Bacabac, R.G.; Klein-Nulend, J. Cellulose and its derivatives: Towards biomedical applications. *Cellulose* **2021**, *28*, 1893–1931. [[CrossRef](#)]
10. Menon, M.P.; Selvakumar, R.; Sureshkumar, P.; Ramakrishna, S. Extraction and modification of cellulose nanofibers derived from biomass for environmental application. *RSC Adv.* **2017**, *7*, 42750–42773. [[CrossRef](#)]
11. Wang, Z.; Lee, Y.H.; Kim, S.W.; Seo, J.Y.; Lee, S.Y.; Nyholm, L. Why Cellulose-Based Electrochemical Energy Storage Devices? *Adv. Mater.* **2021**, *33*, e2000892. [[CrossRef](#)]
12. Calle-Gil, R.; Castillo-Martínez, E.; Carretero-González, J. Cellulose Nanocrystals in Sustainable Energy Systems. *Adv. Sustain. Syst.* **2022**, *6*, 2100395. [[CrossRef](#)]
13. Sheng, J.; Tong, S.; He, Z.; Yang, R. Recent developments of cellulose materials for lithium-ion battery separators. *Cellulose* **2017**, *24*, 4103–4122. [[CrossRef](#)]
14. Mayilswamy, N.; Kandasubramanian, B. Green composites prepared from soy protein, polylactic acid (PLA), starch, cellulose, chitin: A review. *Emergent Mater.* **2022**, *5*, 727–753. [[CrossRef](#)]
15. Li, C.; Sun, Y.; Yi, Z.; Zhang, L.; Zhang, S.; Hu, X. Co-pyrolysis of coke bottle wastes with cellulose, lignin and sawdust: Impacts of the mixed feedstock on char properties. *Renew. Energy* **2022**, *181*, 1126–1139. [[CrossRef](#)]
16. Abe, K.; Yano, H. Comparison of the characteristics of cellulose microfibril aggregates isolated from fiber and parenchyma cells of Moso bamboo (*Phyllostachys pubescens*). *Cellulose* **2009**, *17*, 271–277. [[CrossRef](#)]
17. Paakko, M.; Ankerfors, M.; Kosonen, H.; Nykanen, A.; Ahola, S.; Osterberg, M.; Ruokolainen, J.; Laine, J.; Larsson, P.T.; Ikkala, O.; et al. Enzymatic hydrolysis combined with mechanical shearing and high-pressure homogenization for nanoscale cellulose fibrils and strong gels. *Biomacromolecules* **2007**, *8*, 1934–1941. [[CrossRef](#)] [[PubMed](#)]
18. Okita, Y.; Saito, T.; Isogai, A. Entire surface oxidation of various cellulose microfibrils by TEMPO-mediated oxidation. *Biomacromolecules* **2010**, *11*, 1696–1700. [[CrossRef](#)]
19. Cao, D.X.; Xing, Y.J.; Tantratian, K.; Wang, X.; Ma, Y.; Mukhopadhyay, A.; Cheng, Z.; Zhang, Q.G.; Jiao, Y.; Chen, L.; et al. 3D Printed High-Performance Lithium Metal Microbatteries Enabled by Nanocellulose. *Adv. Mater.* **2019**, *31*, 1807313. [[CrossRef](#)]
20. Pennells, J.; Godwin, I.D.; Amiralian, N.; Martin, D.J. Trends in the production of cellulose nanofibers from non-wood sources. *Cellulose* **2019**, *27*, 575–593. [[CrossRef](#)]
21. Hassan, M.; Berglund, L.; Hassan, E.; Abou-Zeid, R.; Oksman, K. Effect of xylanase pretreatment of rice straw unbleached soda and neutral sulfite pulps on isolation of nanofibers and their properties. *Cellulose* **2018**, *25*, 2939–2953. [[CrossRef](#)]
22. Song, Y.; Jiang, W.; Zhang, Y.; Ben, H.; Han, G.; Ragauskas, A.J. Isolation and characterization of cellulosic fibers from kenaf bast using steam explosion and Fenton oxidation treatment. *Cellulose* **2018**, *25*, 4979–4992. [[CrossRef](#)]
23. Zhao, G.; Du, J.; Chen, W.; Pan, M.; Chen, D. Preparation and thermostability of cellulose nanocrystals and nanofibrils from two sources of biomass: Rice straw and poplar wood. *Cellulose* **2019**, *26*, 8625–8643. [[CrossRef](#)]
24. Zhang, K.; Zheng, S.; Liu, Y.; Lin, J. Isolation of hierarchical cellulose building blocks from natural flax fibers as a separation membrane barrier. *Int. J. Biol. Macromol.* **2020**, *155*, 666–673. [[CrossRef](#)] [[PubMed](#)]
25. Petroudy, S.R.D.; Chabot, B.; Loranger, E.; Naebe, M.; Shojaeiarani, J.; Gharehkhani, S.; Ahvazi, B.; Hu, J.; Thomas, S. Recent Advances in Cellulose Nanofibers Preparation through Energy-Efficient Approaches: A Review. *Energies* **2021**, *14*, 6792. [[CrossRef](#)]
26. Baati, R.; Mabrouk, A.B.; Magnin, A.; Boufi, S. CNFs from twin screw extrusion and high pressure homogenization: A comparative study. *Carbohydr. Polym.* **2018**, *195*, 321–328. [[CrossRef](#)]
27. Hongrattanavichit, I.; Aht-Ong, D. Nanofibrillation and characterization of sugarcane bagasse agro-waste using water-based steam explosion and high-pressure homogenization. *J. Clean. Prod.* **2020**, *277*, 123471. [[CrossRef](#)]
28. Arantes, V.; Dias, I.K.R.; Berto, G.L.; Pereira, B.; Marotti, B.S.; Nogueira, C.F.O. The current status of the enzyme-mediated isolation and functionalization of nanocelluloses: Production, properties, techno-economics, and opportunities. *Cellulose* **2020**, *27*, 10571–10630. [[CrossRef](#)]
29. Sanchez-Salvador, J.L.; Campano, C.; Balea, A.; Tarres, Q.; Delgado-Aguilar, M.; Mutje, P.; Blanco, A.; Negro, C. Critical comparison of the properties of cellulose nanofibers produced from softwood and hardwood through enzymatic, chemical and mechanical processes. *Int. J. Biol. Macromol.* **2022**, *205*, 220–230. [[CrossRef](#)]
30. Yamato, K.; Yoshida, Y.; Kumamoto, Y.; Isogai, A. Surface modification of TEMPO-oxidized cellulose nanofibers, and properties of their acrylate and epoxy resin composite films. *Cellulose* **2021**, *29*, 2839–2853. [[CrossRef](#)]
31. Koochi, H.; Intyre, J.M.; Viitanen, L.; Puisto, A.; Maleki-Jirsaraei, N.; Alava, M. Local time-dependent microstructure of aging TEMPO nanofibrillated cellulose gel. *Cellulose* **2022**, *30*, 61–74. [[CrossRef](#)]
32. Isogai, A.; Kato, Y. Preparation of polyuronic acid from cellulose by TEMPO-mediated oxidation. *Cellulose* **1998**, *5*, 153–164. [[CrossRef](#)]

33. Delgado-Aguilar, M.; Tarrés, Q.; Puig, J.; Boufi, S.; Blanco, Á.; Mutjé, P. Enzymatic Refining and Cellulose Nanofiber Addition in Papermaking Processes from Recycled and Deinked Slurries. *BioResources* **2015**, *10*, 5730–5743. [[CrossRef](#)]
34. Alila, S.; Besbes, I.; Vilar, M.R.; Mutjé, P.; Boufi, S. Non-woody plants as raw materials for production of microfibrillated cellulose (MFC): A comparative study. *Ind. Crops Prod.* **2013**, *41*, 250–259. [[CrossRef](#)]
35. Tarrés, Q.; Boufi, S.; Mutjé, P.; Delgado-Aguilar, M. Enzymatically hydrolyzed and TEMPO-oxidized cellulose nanofibers for the production of nanopapers: Morphological, optical, thermal and mechanical properties. *Cellulose* **2017**, *24*, 3943–3954. [[CrossRef](#)]
36. Patterson, G.; Hsieh, Y.L. Tunable dialdehyde/dicarboxylate nanocelluloses by stoichiometrically optimized sequential periodate-chlorite oxidation for tough and wet shape recoverable aerogels. *Nanoscale Adv.* **2020**, *2*, 5623–5634. [[CrossRef](#)]
37. Sun, X.; He, Q.; Yang, Y. Preparation of Dicarboxyl Cellulose Nanocrystals from Agricultural Wastes by Sequential Periodate-Chlorite Oxidation. *J. Renew. Mater.* **2020**, *8*, 447–460. [[CrossRef](#)]
38. Butchosa, N.; Zhou, Q. Water redispersible cellulose nanofibrils adsorbed with carboxymethyl cellulose. *Cellulose* **2014**, *21*, 4349–4358. [[CrossRef](#)]
39. Azrak, S.M.E.A.; Gohl, J.A.; Moon, R.J.; Schueneman, G.T.; Davis, C.S.; Youngblood, J.P. Controlled Dispersion and Setting of Cellulose Nanofibril—Carboxymethyl Cellulose Pastes. *Cellulose* **2021**, *28*, 9149–9168. [[CrossRef](#)]
40. Wagberg, L.; Decher, G.; Norgren, M.; Lindstrom, T.; Ankerfors, M.; Axnas, K. The build-up of polyelectrolyte multilayers of microfibrillated cellulose and cationic polyelectrolytes. *Langmuir* **2008**, *24*, 784–795. [[CrossRef](#)]
41. Chen, W.; Li, Q.; Wang, Y.; Yi, X.; Zeng, J.; Yu, H.; Liu, Y.; Li, J. Comparative study of aerogels obtained from differently prepared nanocellulose fibers. *ChemSusChem* **2014**, *7*, 154–161. [[CrossRef](#)]
42. Ifuku, S.; Nogi, M.; Abe, K.; Handa, K.; Nakatsubo, F.; Yano, H. Surface modification of bacterial cellulose nanofibers for property enhancement of optically transparent composites: Dependence on acetyl-group DS. *Biomacromolecules* **2007**, *8*, 1973–1978. [[CrossRef](#)] [[PubMed](#)]
43. Zhong, X.; Han, J.; Chen, L.; Liu, W.; Jiao, F.; Zhu, H.; Qin, W. Binding mechanisms of PVDF in lithium ion batteries. *Appl. Surf. Sci.* **2021**, *553*, 149564. [[CrossRef](#)]
44. Wu, Y.; Li, Y.; Wang, Y.; Liu, Q.; Chen, Q.; Chen, M. Advances and prospects of PVDF based polymer electrolytes. *J. Energy Chem.* **2022**, *64*, 62–84. [[CrossRef](#)]
45. Yang, B.; Guo, D.; Lin, P.; Zhou, L.; Li, J.; Fang, G.; Wang, J.; Jin, H.; Chen, X.A.; Wang, S. Hydroxylated Multi-Walled Carbon Nanotubes Covalently Modified with Tris(hydroxypropyl) Phosphine as a Functional Interlayer for Advanced Lithium-Sulfur Batteries. *Angew. Chem.* **2022**, *61*, e202204327.
46. Darjazi, H.; Staffolani, A.S.; Sbrascini, L.; Bottoni, L.; Tossici, R.; Nobili, F. Sustainable Anodes for Lithium- and Sodium-Ion Batteries Based on Coffee Ground-Derived Hard Carbon and Green Binders. *Energies* **2020**, *13*, 6216. [[CrossRef](#)]
47. Lee, J.-H.; Lee, S.; Paik, U.; Choi, Y.-M. Aqueous processing of natural graphite particulates for lithium-ion battery anodes and their electrochemical performance. *J. Power Sources* **2005**, *147*, 249–255. [[CrossRef](#)]
48. Kwon, T.W.; Choi, J.W.; Coskun, A. The emerging era of supramolecular polymeric binders in silicon anodes. *Chem. Soc. Rev.* **2018**, *47*, 2145–2164. [[CrossRef](#)] [[PubMed](#)]
49. Tian, W.; VahidMohammadi, A.; Reid, M.S.; Wang, Z.; Ouyang, L.; Erlandsson, J.; Pettersson, T.; Wagberg, L.; Beidaghi, M.; Hamed, M.M. Multifunctional Nanocomposites with High Strength and Capacitance Using 2D MXene and 1D Nanocellulose. *Adv. Mater.* **2019**, *31*, e1902977. [[CrossRef](#)]
50. Lu, H.; Behm, M.; Leijonmarck, S.; Lindbergh, G.; Cornell, A. Flexible Paper Electrodes for Li-Ion Batteries Using Low Amount of TEMPO-Oxidized Cellulose Nanofibrils as Binder. *ACS Appl. Mater. Interfaces* **2016**, *8*, 18097–18106. [[CrossRef](#)]
51. Lu, H.; Guccini, V.; Kim, H.; Salazar-Alvarez, G.; Lindbergh, G.; Cornell, A. Effects of Different Manufacturing Processes on TEMPO-Oxidized Carboxylated Cellulose Nanofiber Performance as Binder for Flexible Lithium-Ion Batteries. *ACS Appl. Mater. Interfaces* **2017**, *9*, 37712–37720. [[CrossRef](#)] [[PubMed](#)]
52. Wu, J.; Zhang, Q.; Liu, S.; Long, J.; Wu, Z.; Zhang, W.; Pang, W.K.; Sencadas, V.; Song, R.; Song, W.; et al. Synergy of binders and electrolytes in enabling microsized alloy anodes for high performance potassium-ion batteries. *Nano Energy* **2020**, *77*, 105118. [[CrossRef](#)]
53. Rajeevan, S.; John, S.; George, S.C. Polyvinylidene fluoride: A multifunctional polymer in supercapacitor applications. *J. Power Sources* **2021**, *504*, 230037. [[CrossRef](#)]
54. Aslan, M.; Weingarh, D.; Jäckel, N.; Atchison, J.S.; Grobelsek, I.; Presser, V. Polyvinylpyrrolidone as binder for castable supercapacitor electrodes with high electrochemical performance in organic electrolytes. *J. Power Sources* **2014**, *266*, 374–383. [[CrossRef](#)]
55. Daraghme, A.; Hussain, S.; Servera, L.; Xuriguera, E.; Cornet, A.; Cirera, A. Impact of binder concentration and pressure on performance of symmetric CNFs based supercapacitors. *Electrochim. Acta* **2017**, *245*, 531–538. [[CrossRef](#)]
56. Lacey, M.J.; Jeschull, F.; Edström, K.; Brandell, D. Porosity Blocking in Highly Porous Carbon Black by PVdF Binder and Its Implications for the Li-S System. *J. Phys. Chem. C* **2014**, *118*, 25890–25898. [[CrossRef](#)]
57. Rabuni, M.F.; Sulaiman, N.M.N.; Aroua, M.K.; Hashim, N.A. Effects of Alkaline Environments at Mild Conditions on the Stability of PVDF Membrane: An Experimental Study. *Ind. Eng. Chem. Res.* **2013**, *52*, 15874–15882. [[CrossRef](#)]
58. Mian, M.M.; Kamana, I.M.L.; An, X.; Abbas, S.C.; Ahommed, M.S.; He, Z.; Ni, Y. Cellulose nanofibers as effective binders for activated biochar-derived high-performance supercapacitors. *Carbohydr. Polym.* **2023**, *301*, 120353. [[CrossRef](#)]

59. Jabbour, L.; Bongiovanni, R.; Chaussy, D.; Gerbaldi, C.; Beneventi, D. Cellulose-based Li-ion batteries: A review. *Cellulose* **2013**, *20*, 1523–1545. [[CrossRef](#)]
60. Xiao, S.Y.; Yang, Y.Q.; Li, M.X.; Wang, F.X.; Chang, Z.; Wu, Y.P.; Liu, X. A composite membrane based on a biocompatible cellulose as a host of gel polymer electrolyte for lithium ion batteries. *J. Power Sources* **2014**, *270*, 53–58. [[CrossRef](#)]
61. Wang, S.; Zhang, L.; Zeng, Q.; Liu, X.; Lai, W.-Y.; Zhang, L. Cellulose Microcrystals with Brush-Like Architectures as Flexible All-Solid-State Polymer Electrolyte for Lithium-Ion Battery. *ACS Sustain. Chem. Eng.* **2020**, *8*, 3200–3207. [[CrossRef](#)]
62. Qu, S.; Liu, J.; Han, X.; Deng, Y.; Zhong, C.; Hu, W. Dynamic stretching–electroplating metal-coated textile for a flexible and stretchable zinc–air battery. *Carbon Energy* **2022**, *4*, 867–877. [[CrossRef](#)]
63. Hui, X.; Zhang, P.; Li, J.; Zhao, D.; Li, Z.; Zhang, Z.; Wang, C.; Wang, R.; Yin, L. In Situ Integrating Highly Ionic Conductive LDH-Array@PVA Gel Electrolyte and MXene/Zn Anode for Dendrite-Free High-Performance Flexible Zn–Air Batteries. *Adv. Energy Mater.* **2022**, *12*, 2201393. [[CrossRef](#)]
64. Abrial, H.; Atmajaya, A.; Mahardika, M.; Hafizulhaq, F.; Kadriadi; Handayani, D.; Sapuan, S.M.; Ilyas, R.A. Effect of ultrasonication duration of polyvinyl alcohol (PVA) gel on characterizations of PVA film. *J. Mater. Res. Technol.* **2020**, *9*, 2477–2486. [[CrossRef](#)]
65. Zhang, Q.; Li, C.; Li, Q.; Pan, Z.; Sun, J.; Zhou, Z.; He, B.; Man, P.; Xie, L.; Kang, L.; et al. Flexible and High-Voltage Coaxial-Fiber Aqueous Rechargeable Zinc-Ion Battery. *Nano Lett.* **2019**, *19*, 4035–4042. [[CrossRef](#)]
66. Huang, Q.; Yang, Y.; Chen, R.; Wang, X. High performance fully paper-based all-solid-state supercapacitor fabricated by a papermaking process with silver nanoparticles and reduced graphene oxide-modified pulp fibers. *EcoMat* **2021**, *3*, e12076. [[CrossRef](#)]
67. Blanc, L.E.; Kundu, D.; Nazar, L.F. Scientific Challenges for the Implementation of Zn-Ion Batteries. *Joule* **2020**, *4*, 771–799. [[CrossRef](#)]
68. Zhou, J.; Zhang, R.; Xu, R.; Li, Y.; Tian, W.; Gao, M.; Wang, M.; Li, D.; Liang, X.; Xie, L.; et al. Super-Assembled Hierarchical Cellulose Aerogel-Gelatin Solid Electrolyte for Implantable and Biodegradable Zinc Ion Battery. *Adv. Funct. Mater.* **2022**, *32*, 2111406. [[CrossRef](#)]
69. Wu, M.L.; Zhang, Y.; Xu, L.; Yang, C.P.; Hong, M.; Cui, M.J.; Clifford, B.C.; He, S.M.; Jing, S.H.; Yao, Y.; et al. A sustainable chitosan-zinc electrolyte for high-rate zinc-metal batteries. *Matter* **2022**, *5*, 3402–3416. [[CrossRef](#)]
70. Xu, L.; Meng, T.T.; Zheng, X.Y.; Li, T.Y.; Brozena, A.H.; Mao, Y.M.; Zhang, Q.; Clifford, B.C.; Rao, J.C.; Hu, L.B. Nanocellulose-Carboxymethylcellulose Electrolyte for Stable, High-Rate Zinc-Ion Batteries. *Adv. Funct. Mater.* **2023**, *33*, 2302098. [[CrossRef](#)]
71. Yu, L.; Fan, Z.; Shao, Y.; Tian, Z.; Sun, J.; Liu, Z. Versatile N-Doped MXene Ink for Printed Electrochemical Energy Storage Application. *Adv. Energy Mater.* **2019**, *9*, 1901839. [[CrossRef](#)]
72. Wei, C.; Tian, M.; Fan, Z.; Yu, L.; Song, Y.; Yang, X.; Shi, Z.; Wang, M.; Yang, R.; Sun, J. Concurrent realization of dendrite-free anode and high-loading cathode via 3D printed N-Ti₃C₂ MXene framework toward advanced Li–S full batteries. *Energy Storage Mater.* **2021**, *41*, 141–151. [[CrossRef](#)]
73. Wady, P.; Wasilewski, A.; Brock, L.; Edge, R.; Baidak, A.; McBride, C.; Leay, L.; Griffiths, A.; Vallés, C. Effect of ionising radiation on the mechanical and structural properties of 3D printed plastics. *Addit. Manuf.* **2020**, *31*, 100907. [[CrossRef](#)]
74. Aeby, X.; Poulin, A.; Siqueira, G.; Hausmann, M.K.; Nystrom, G. Fully 3D Printed and Disposable Paper Supercapacitors. *Adv. Mater.* **2021**, *33*, e2101328. [[CrossRef](#)]
75. Seoane-Viano, I.; Januskaite, P.; Alvarez-Lorenzo, C.; Basit, A.W.; Goyanes, A. Semi-solid extrusion 3D printing in drug delivery and biomedicine: Personalised solutions for healthcare challenges. *J. Control. Release* **2021**, *332*, 367–389. [[CrossRef](#)]
76. Tan, H.W.; An, J.; Chua, C.K.; Tran, T. Metallic Nanoparticle Inks for 3D Printing of Electronics. *Adv. Electron. Mater.* **2019**, *5*, 1800831. [[CrossRef](#)]
77. Liu, H.; Zhang, H.; Han, W.; Lin, H.; Li, R.; Zhu, J.; Huang, W. 3D Printed Flexible Strain Sensors: From Printing to Devices and Signals. *Adv. Mater.* **2021**, *33*, e2004782. [[CrossRef](#)]
78. Qiu, L.; Shao, Z.; Wang, D.; Wang, W.; Wang, F.; Wang, J. Enhanced electrochemical properties of LiFePO₄ (LFP) cathode using the carboxymethyl cellulose lithium (CMC-Li) as novel binder in lithium-ion battery. *Carbohydr. Polym.* **2014**, *111*, 588–591. [[CrossRef](#)]
79. Park, J.S.; Kim, T.; Kim, W.S. Conductive Cellulose Composites with Low Percolation Threshold for 3D Printed Electronics. *Sci. Rep.* **2017**, *7*, 3246. [[CrossRef](#)]
80. Zhou, G.; Li, M.C.; Liu, C.; Wu, Q.; Mei, C. 3D Printed Ti₃C₂T_x MXene/Cellulose Nanofiber Architectures for Solid-State Supercapacitors: Ink Rheology, 3D Printability, and Electrochemical Performance. *Adv. Funct. Mater.* **2022**, *32*, 2109593. [[CrossRef](#)]

Disclaimer/Publisher’s Note: The statements, opinions and data contained in all publications are solely those of the individual author(s) and contributor(s) and not of MDPI and/or the editor(s). MDPI and/or the editor(s) disclaim responsibility for any injury to people or property resulting from any ideas, methods, instructions or products referred to in the content.